Front. Environ. Sci. Eng. 2022, 16(11): 143
https://doi.org/10.1007/s11783-022-1578-8

RESEARCH ARTICLE

V-shaped substrate for surface and volume enhanced Raman spectroscopic analysis of microplastics

Juan Liu[1], Guanjun Xu[1], Xuejun Ruan[1], Kejian Li[1], Liwu Zhang (✉)[1,2]

1 Shanghai Key Laboratory of Atmospheric Particle Pollution and Prevention, Department of Environmental Science & Engineering, Fudan University, Shanghai 200433, China
2 Shanghai Institute of Pollution Control and Ecological Security, Shanghai 200092, China

HIGHLIGHTS

- V-shaped substrate was obtained for SERS analysis of microplastics (diameter ≈ 1 μm).
- Enhancement factor of V-shaped substrate can reach 20 in microplastics detection.
- V-shaped nanopore array can bring additional volume enhancement.
- V-shaped substrate was more economic in application compared to Klarite substrate.

GRAPHIC ABSTRACT

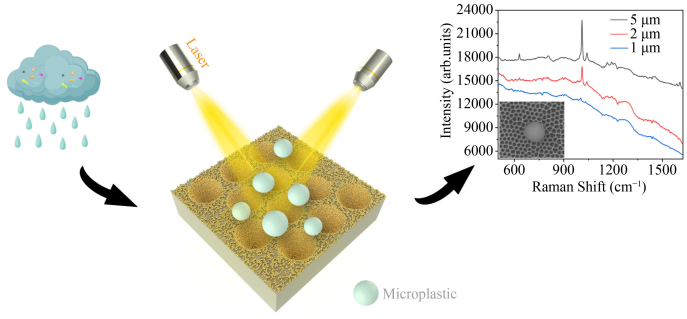

ARTICLE INFO

Article history:
Received 4 January 2022
Revised 17 April 2022
Accepted 22 April 2022
Available online 6 June 2022

Keywords:
SERS
V-shaped
AAO
Microplastic
Atmospheric aerosol

ABSTRACT

Research on the microplastics (MPs) is developing towards smaller size, but corresponding methods for the rapid and accurate detection of microplastics, especially nanoplastics still present challenge. In this work, a novel surface and volume enhanced Raman spectroscopy substrate was developed for the rapid detection of microplastic particles below 5 μm. The gold nanoparticles (NPs) were deposited onto the surface and into the V-shaped nanopores of anodized aluminum oxide (AAO) through magnetron sputtering or ion sputtering, and then AuNPs@V-shaped AAO SERS substrate was obtained and studied for microplastic detection. SERS performance of AuNPs@V-shaped AAO SERS substrate was evaluated through the detection of polystyrene and polymethyl methacrylate microspheres. Results indicated that individual polystyrene sphere with a diameter of 1 μm can be well detected on AuNPs@V-shaped AAO SERS substrate, and the maximum enhancement factor (EF) can reach 20. In addition, microplastics in ambient atmospheric samples were collected and tested to verify the effectiveness of the AuNPs@V-shaped AAO SERS substrate in the real environment. This study provides a rapid, economic and simple method for detecting and identifying microplastics with small size.

1 Introduction

Microplastics are generally defined as pieces of plastics smaller than 5 mm (Thompson et al., 2004). Due to the extensive use of plastics with strong stability and low degradation rates, microplastics are widely found in the environment. Microplastics have been found in marine systems (Law and Thompson, 2014), terrestrial systems (Rillig and Lehmann, 2020), freshwater systems (Koelmans et al., 2019) such as lakes, rivers, and atmospheric systems (Zhu et al., 2021), and even in remote and polar regions (Bergmann et al., 2017; Tekman et al., 2020). Negative impact of microplastics on the environment and creatures should not be underestimated. According to some reported results, microplastics have impact on aquatic organisms (Huang et al., 2021), microorganisms (Seeley et al., 2020), humans and so on. Once microplastics are ingested by organisms, they may cause serious physiological threats, including inflammation, growth retardation, oxidative stress and other symptoms (Wang

✉ Corresponding author
E-mail: zhanglw@fudan.edu.cn

et al., 2021). In addition, microplastics may also become carriers of other pollutants and pathogens (Foulon et al., 2016; Koelmans et al., 2016), posing new risks. Through the transfer and bioaccumulation of food chains, microplastics may eventually become a potential hazard in the human body (Mohamed Nor et al., 2021). Some studies have confirmed that microplastics appear in human excreta (Schwabl et al., 2019) and placenta (Ragusa et al., 2021). More worryingly, microplastics are further degraded by mechanical wear, photodegradation and biodegradation and then form smaller microplastics with more significant toxicological properties (Wang et al., 2021). But at the same time, the difficulty in detection also increases greatly. Therefore, we urgently need to develop new detection methods which are suitable for the microplastics of smaller size.

In the past decade or so, there has been a significant increase in research and publications on microplastics with a major focus on the aquatic environment, particularly marine systems (Zhang et al., 2020b). However, studies on microplastics in atmospheric environment are still in the early stage. It is a remarkable fact that deposition of microplastics in the atmosphere can be a potential source of microplastics in the aquatic and terrestrial environments (Liu et al., 2019; Huang et al., 2021). In addition, compared with microplastics in other environmental systems, microplastics in the atmosphere can be directly and continuously inhaled into the human body, posing potential health risks (Chen et al., 2020; Zhang et al., 2020a). To some extent, intake of microplastics through atmosphere is more frequent than contaminant food (Catarino et al., 2018). Therefore, it is necessary to pay attention to the detection of microplastics in atmospheric environment.

To date, methods for microplastics detection include pyrolysis gas chromatography-mass spectrometry (Py-GC-MS) (Hendrickson et al., 2018), Fourier transform infrared spectroscopy (FTIR) (Hendrickson et al., 2018), liquid chromatography-tandem mass spectrometry (LC-MS/MS) (Wang et al., 2017), Raman spectroscopy (Araujo et al., 2018), etc. However, the smallest detectable size of these technologies has only reached around 10 μm so far. Therefore, those detection methods are far from meeting the needs of current and future research. Surface enhanced Raman scattering (SERS) is a technology based on conventional Raman spectroscopy. Generally, the Raman scattering of molecules is weak. However, when the molecules are adsorbed on the rough surface of noble metals such as gold and silver, the Raman scattering of molecules will be significantly enhanced. Even high sensitivity at the single-molecule level can be achieved (Langer et al., 2020; Wang et al., 2020). Due to its excellent properties, SERS technique has been widely used in environmental analysis, food safety, biomedical analysis and other fields (Lv et al., 2020; Lê et al., 2021). In our previous work, we have realized detection of nanoplastics via a commercial SERS substrate–Klarite (Xu et al., 2020), however, the high cost of Klarite making it unsuitable for large amount application. There is urgent need to develop SERS substrates with low cost for microplastics detection.

Nanostructure-related SERS techniques have been widely employed in environmental research. It is a simple, rapid and efficient method to apply templates for developing SERS substrates. Compared to other templates with nanostructure, anodic aluminum oxide (AAO) templates are widely adopted because of their highly uniform nanoporous structure (Nagaura et al., 2008). After combining with the noble metal materials (gold or silver), AAO templates will form a large number of high-density "hot spots", which exhibit high SERS sensitivity (He et al., 2019; Shi et al., 2019). In addition, the three-dimensional ordered nanoporous structure can expand the specific surface area for the adsorption of analyte molecules (Shi et al., 2019). Therefore, we chose AAO as the template to prepare SERS substrate for the detection of microplastics.

In this work, an SERS substrate for the detection of small-size microplastics was developed. V-shaped AAO template has a large number of ordered inverted cone-shaped nanopores. Gold nanoparticles were deposited on the surface and into these nanopores by magnetron sputtering or ion sputtering, and then AuNPs@V-shaped AAO SERS substrate was obtained. Due to the porous properties of the V-shaped AAO template, this novel AuNPs@V-shaped AAO SERS substrate could provide substantial "hot spots", which exhibit high SERS sensitivity in detecting microplastics. Polystyrene (PS) and polymethyl methacrylate (PMMA) standard samples were tested on this SERS substrate to evaluate its ability, and the corresponding enhancement factor was calculated. In addition, the SERS performance between substrates formed by magnetron sputtering and ion sputtering were studied and compared. The potential of this substrate for application in the real environment was tested by detecting microplastics in the collected rainwater samples.

2 Materials and methods

2.1 Materials

V-shaped AAO template with a size of 20 mm × 20 mm was purchased from Shenzhen Topology Film Co., Ltd, China. PS and PMMA microsphere suspension of different sizes were purchased from Shanghai Huge Biotechnology Co., Ltd, China. PS microspheres involved three sizes of 1 μm, 2 μm, and 5 μm, and PMMA microspheres involved two sizes of 1 μm, 2 μm. All sizes of PS and PMMA microsphere suspension were supplied as 5% (w/v) monodispersed in deionized water. Glass pipette

(NICHIRYO Nichipet ECO, Japan) was purchased from Zeal Quest Equipments Co., Ltd, China. Deionized water (18.3 MΩ) and absolute ethanol were used throughout the experiment.

2.2 Fabrication and characterization of AuNPs@V-shaped AAO SERS substrate

V-shaped AAO template was first cleaned ultrasonically in deionized water, then dried it in air before use. AuNPs@V-shaped AAO SERS substrate was prepared by magnetron sputtering (DE500, Alliance Concept, France) and ion sputtering (GVC-1000, GEVEE, China) to deposit gold nanoparticles, and thickness of gold nanoparticles layer was optimized and set to 50 nm. The fabrication process of the AuNPs@V-shaped AAO SERS substrate was displayed in Fig. 1. In addition, morphological characterization and energy dispersive spectrometer analysis were conducted by scanning electron microscopy (SEM) (VEGA 3, TESCAN, China) with 15 kV accelerating voltage, unless otherwise mentioned.

2.3 Standard microplastics sample preparation

PS and PMMA standard microsphere suspensions were fully diluted with deionized water to a ratio of 1:4 in the volume of 4 mL to obtain individual particles, respectively. The mass density of the PS material is 1.05 g/cm^3 and PMMA material is 1.18 g/cm^3. The final concentration of diluted standard samples was 2.625 × 10^{-5} g/cm^3 for PS and 2.950 × 10^{-5} g/cm^3 for PMMA. Herein, 5 μL of each diluted microsphere suspension was dropped onto AuNPs@V-shaped AAO SERS substrate and silicon wafer by glass pipette, respectively, and dried in the nitrogen.

2.4 Raman measurement and data analysis

SERS analysis was conducted by an XploRA Plus confocal Raman spectrometer (Jobin Yvon, Horiba Gr, France) equipped with a multi-channel electron multiplying charge-coupled detector (EMCCD) device upon 1200 lines per mm grating, which was calibrated according to the 520 cm^{-1} Raman spectra of the silicon wafer. Microplastic microspheres were observed under a ×100 optical microscope objective lens (Olympus, 0.90 Numerical Aperture, Japan) and excited by a 785 nm laser at a power of 25 mW. The Raman spectra were collected in the range of 200–2000 cm^{-1}, with 15 s acquisition time for the standard sample and 50 s acquisition time for atmospheric aerosol sample at 5 spectra accumulations per second. All data were processed through commercial softwares LabSpec 6.0 and Origin 2018 version.

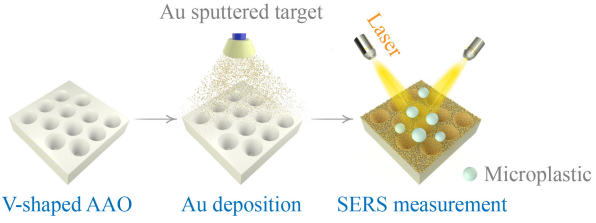

Fig. 1 Schematic illustration of the fabrication process of the AuNPs@V-shaped AAO SERS substrate and SERS measurement by Raman system.

2.5 Collection and treatment of microplastics in rainwater

Microplastic particles in the atmosphere fall under the scouring and carrying of the rainwater when it rains. In this work, we equated the process of collecting rainwater with dispersing atmospheric particulates into an aqueous solution under natural conditions. From this perspective, we studied the rainwater samples as atmospheric samples. Rainwater was collected in cleaned glass container at Fudan University. Collected rainwater was first filtered with a 10 μm diameter glass fiber filter and the filter was ultrasonically cleaned in deionized water to obtain the particles. In order to reduce the interference of organic, biological and other non-plastic substances, hydrogen peroxide (H_2O_2) solution (30%) was added into the solution involving particles obtained in the previous process for treatment for 24 h at room temperature. Digestion of rainwater samples with H_2O_2 can remove organic matters and reduce the interference of fluorescence. The solution was filtered with a 1 μm diameter glass fiber filter subsequently and particles on the filter were sonicated into deionized water. Finally, the solution was heated to 50 °C for concentration in a clean glass container and transferred to AuNPs@V-shaped AAO SERS substrate through a glass pipette. During the whole process, interferences that came from equipments and the lab were avoid to the utmost by keeping covering glass container with clean glass, wearing cotton lab coat and covering samplers with aluminum foil.

3 Results and discussion

3.1 Structure and morphology characterization of AuNPs@V-shaped AAO SERS substrate

Figure 2(a) shows the SEM image of initial bare V-shaped AAO template. AuNPs@V-shaped AAO SERS substrate was prepared in the process shown in Fig. 1, and then characterized with SEM. AuNPs were deposited on V-shaped AAO template with magnetron sputtering or ion sputtering. Figures 2(b) and 2(c) show the top-view SEM images of AuNPs@V-shaped AAO SERS substrate formed by ion sputtering and magnetron sputtering, respectively. Compared to initial bare V-shaped AAO

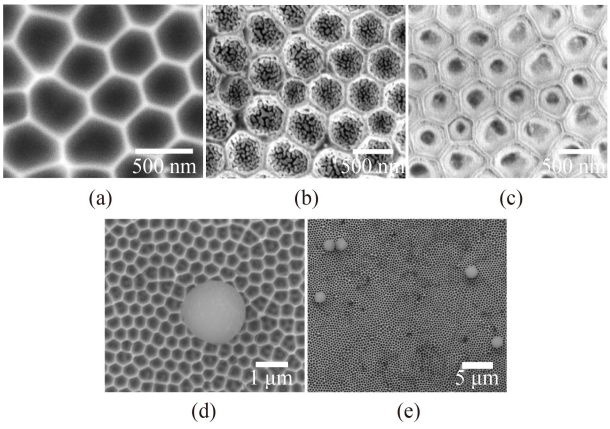

Fig. 2 Top-view SEM images of bare AAO template (a), AuNPs@V-shaped AAO SERS substrate, which was obtained through ion sputtering (b) and magnetron sputtering (c), respectively, and PS microspheres (diameter = 2 μm) on AuNPs@V-shaped AAO SERS substrate in different magnifications (d, e).

template, it is clearly indicated that AuNPs were effectively deposited inside the nanopores and on the surface of V-shaped AAO template in a uniform form, which produced a strong SERS effect. Three-dimensional nanoporous structure can not only provide more "hot spots", but also stimulate stronger electromagnetic field enhancement. The nanopores of V-shaped AAO template were inverted cones. The average top diameter was 400 nm, the average depth was 400 nm, and the average bottom diameter was 100 nm. In addition, by comparing Figs. 2(b) and 2(c), we can find that the morphologies of AuNPs formed by magnetron sputtering and ion sputtering are significantly different, which leads to differences in subsequent Raman detection results. Figures 2(d) and 2(e) show the distribution of microplastic microspheres on the substrate in a single particle manner, which prove that the initial suspensions of microplastic microspheres was sufficiently diluted to realize the Raman detection of individual microplastic sphere. In addition, to demonstrate distributions of chemical elements in the AuNPs@V-shaped AAO nanostructure, energy spectrum and energy-dispersive X-ray spectroscopy (EDS) maps of carbon (yellow) and gold (fuchsia) were obtained (shown in Fig. 3).

3.2 Normal Raman detection of PS

PS is a thermoplastic and one of the most widely used plastic materials. In this work, normal Raman detection of

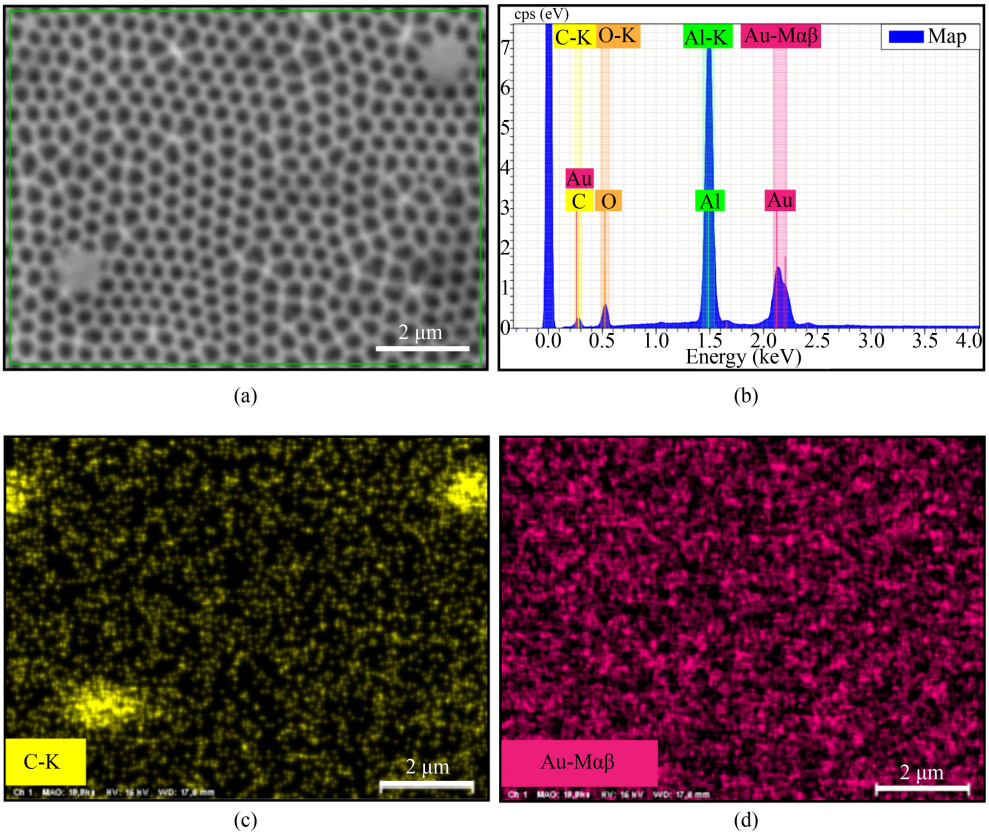

Fig. 3 Energy-dispersive X-ray spectroscopy (EDS) map and energy spectrum of AuNPs@V-shaped AAO SERS substrate with microplastic particles. (a) Scanning area; (b) Energy spectrum of AuNPs@V-shaped AAO, which involved C, O, Al, Au corresponding to the peaks in sequence; (c) The EDS map of C, corresponding to the position of the microplastic particles in the scanning area (a); (d) The EDS map of Au, showing an effective and relatively uniform AuNPs depositing result.

PS microspheres was conducted by silicon wafer. Three standard PS microsphere suspensions containing different sizes of 1 μm, 2 μm and 5 μm respectively were fully diluted and then dripped onto the silicon wafer (a non-SERS substrate). Figure 4(a) shows the Raman spectra of PS microspheres of each size on the silicon wafer, and corresponding optical images of every single PS microsphere are displayed in Fig. 4(b). Each Raman spectra shown in Fig. 4(a) was produced by a single PS microsphere after being excited, which can be proved by Fig. 4(b). The peaks of the silicon wafer at 520 cm^{-1} and 800–1000 cm^{-1} dominated the Raman spectra (Parker et al., 1967). However, the characteristic Raman peaks of PS microspheres can hardly be observed. In previous studies, typical Raman signals of PS were located at 619, 1003, 1033, 1600 cm^{-1}, which can be attributed to the C-C ring breathing mode, the ring deformation mode, the CH- in-plane deformation band and the C-C stretching vibrations, respectively (Anema et al., 2010). According to the Inset, only PS microspheres with sizes of 5 μm and 2 μm

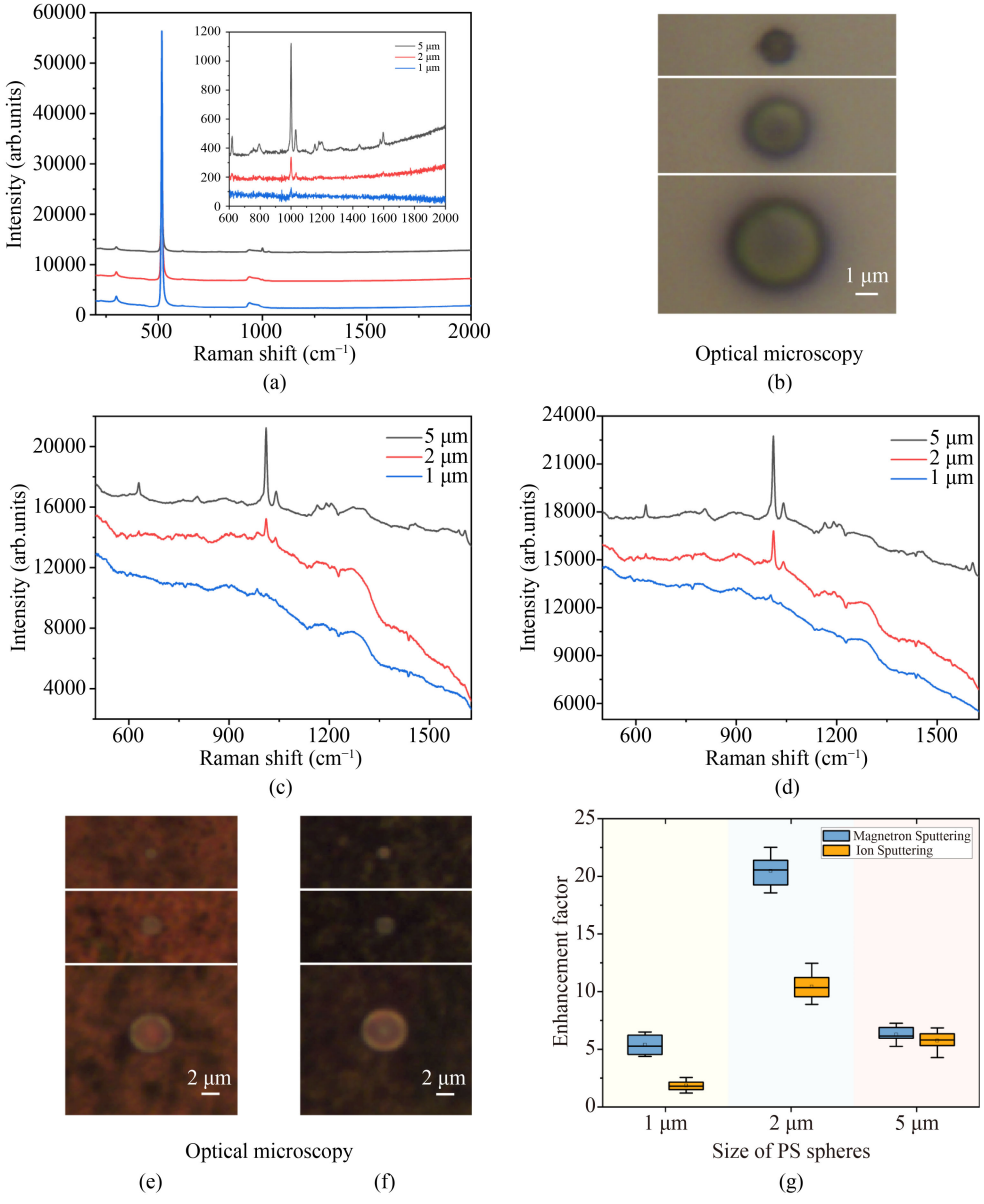

Fig. 4 (a) Raman spectra of PS microspheres of different sizes on silicon wafer (5 spectral acquisitions with 15 s acquisition time) (Inset: spectra from 600 to 2000 cm^{-1}). (b) Optical microscopy images (bright-field microscopy, in reflection) of 1 μm, 2 μm, 5 μm PS microspheres placed on silicon wafer in a single particle manner. (c, d) Raman spectra of PS microspheres of different sizes detected by AuNPs@V-shaped AAO SERS substrate prepared by ion sputtering and magnetron sputtering, respectively. (e, f) Optical microscopy images of 1 μm, 2 μm, 5 μm PS microspheres placed on AuNPs@V-shaped AAO SERS substrate prepared by magnetron sputtering and ion sputtering, respectively. (g) Box and whisker plot of Enhancement Factors of PS microspheres as a function of size.

appeared Raman signals at 1003 cm^{-1} and 1033 cm^{-1} with relatively weak intensity. When the size of PS microspheres was reduced to 1 μm, PS could no longer be detected. Therefore, normal Raman detection is hardly applied for small-size microplastics.

3.3 SERS of PS

The Raman spectra obtained by PS microspheres on two different AuNPs@V-shaped AAO SERS substrate were shown in Figs. 4(c) and 4(d). The two substrates were prepared by two different gold nanoparticles sputtering methods: magnetron sputtering and ion sputtering, respectively. Figures 4(e) and 4(f) respectively show the optical images of PS microspheres on AuNPs@V-shaped AAO SERS substrate prepared in two methods mentioned above. Compared with the silicon wafer, the Raman signal of a single PS microsphere on AuNPs@V-shaped AAO SERS substrate was significantly enhanced due to the surface enhancement effect of rough gold nanoparticles. More significantly, the Raman signal from a single PS microsphere with a size of 1 μm can be detected at 1003 cm^{-1} and 1033 cm^{-1} with relatively strong intensity. In addition, AuNPs@V-shaped AAO SERS substrate can hardly produce additional background interference compared with silicon wafer. It indicated that AuNPs@V-shaped AAO SERS substrate has potential to be applied for microplastics with small sizes, which can be ascribed to the three-dimensional inverted cone-shaped gold nanostructure array with a considerable number of "hot spots".

3.4 SERS analysis of PMMA

PMMA is another common plastic product that is often utilized as an alternative to glass. In order to further investigate the potential of AuNPs@V-shaped AAO SERS substrate in microplastics detection, PMMA was also studied in a single particle manner. PMMA was tested with two sizes of 2 μm and 5 μm, and the processing and Raman measurement were the same as that of PS. Raman spectra and optical microscopy images of PMMA microspheres on silicon wafer were shown in Figs. 5(a) and 5(b), which was consistent with the results of PS that Raman signal of silicon wafer dominated the Raman spectra and PMMA exhibited weak Raman signals.

On the contrary, Figs. 5(c) and 5(d) show the Raman spectra of individual PMMA microspheres on AuNPs@V-shaped AAO SERS substrate prepared by magnetron sputtering and ion sputtering, respectively. They indicated that AuNPs@V-shaped AAO SERS substrate still exhibited stronger Raman signals from PMMA than silicon wafer. According to some literature, main characteristic peaks of PMMA are located at 622, 817, 1000, 1200, 1452 and 1723 cm^{-1}, which can be assigned to C-C-O stretching, C-O-C symmetric stretching, C-C stretching, C-H bending and C=O stretching, respectively (Xu et al., 2020). Figures 5(e) and 5(f) show the corresponding optical microscopy images of individual PMMA microspheres of different sizes on AuNPs@V-shaped AAO SERS substrate. Above all, AuNPs@V-shaped AAO SERS substrate proved to be suitable for different microplastics detection and identification.

3.5 Calculation of enhancement factor

We calculated enhancement factor (*EF*) to quantitatively evaluate the performance of AuNPs@V-shaped AAO SERS substrate. In the literature, EF has many definition, among which the widely acknowledged definition is demonstrated as the following equation (Eq. (1)).

$$EF = \frac{I_{SERS}}{I_{NRS}} \times \frac{N_{NRS}}{N_{SERS}}, \quad (1)$$

where I_{SERS} and I_{NRS} represent the dominant SERS intensities at 1003 cm^{-1} peak of PS microsphere or at 817 cm^{-1} peak of PMMA microsphere on AuNPs@V-shaped AAO SERS substrate and on silicon wafer (non-SERS substrate), respectively. N_{SERS} and N_{NRS} are the number of molecules in the laser spot on SERS substrate and non-SERS substrate, respectively. In this study, we detected a single microplastic sphere on the substrate, so only one molecule appeared in the laser spot. Herein, N_{NRS} and N_{SERS} can be set as 1. In order to eliminate the impact on Raman intensity, accumulation time and laser power were kept constant.

Figures 4(g) and 5(g) demonstrate the calculated EFs of PS and PMMA at a shift of 1003 cm^{-1} and 817 cm^{-1}, respectively. In order to eliminate the impact of fluctuation and keep Raman signals stable, five particles of each size were randomly selected and measured three times. The average EF for PS microspheres with 5 μm was 6.5 for magnetron sputtering and 5.0 for ion sputtering. While the results of 2 μm PS microspheres increased significantly to 20.0 for magnetron sputtering and 10.0 for ion sputtering, the results of 1 μm PS microspheres decreased to 5.0 for magnetron sputtering and 2.0 for ion sputtering. As for PMMA, the average EF of 5 μm microspheres achieved 3.5 for magnetron sputtering and 2.5 for ion sputtering. Consistent with PS, EF of PMMA with a size of 2 μm increased to 8.0 for magnetron sputtering and 6.5 for ion sputtering.

According to the calculation results, EFs have a correlation with the particle size of microplastics. Although both PS and PMMA with a size of 5 μm exhibited the strongest Raman signal, they had no advantage when compared with 2 μm microspheres in EF. However, the EF value of 1 μm PS microsphere decreased significantly. We attribute this phenomenon to the interaction between the volume of the particles and the position of the particles in the nanopores, which are determined by the

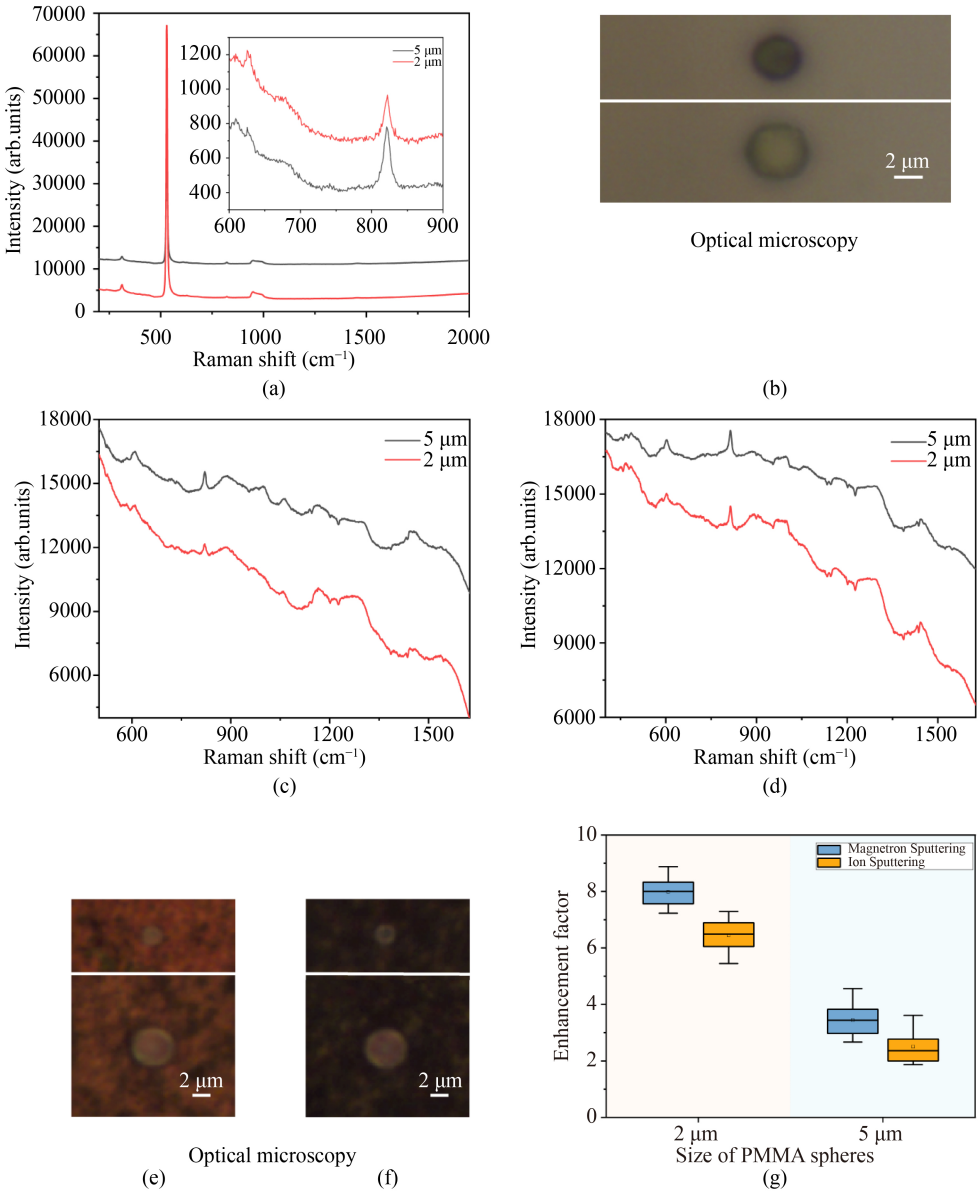

Fig. 5 (a) Raman spectra of PMMA microspheres of different sizes on silicon wafer (5 spectral accumulations with 15 s acquisition time) (Inset: spectra from 600 to 900 cm^{-1}). (b) Optical microscopy images of 2 μm, 5 μm PMMA microspheres placed on silicon wafer in a single particle manner. (c, d) Raman spectra of PMMA microspheres of different sizes detected by AuNPs@V-shaped AAO SERS substrate prepared by ion sputtering and magnetron sputtering, respectively. (e, f) Optical microscopy images of 2 μm, 5 μm PMMA microspheres placed on AuNPs@V-shaped AAO SERS substrate prepared by magnetron sputtering and ion sputtering, respectively. (g) Box and whisker plot of EFs of PMMA microspheres as a function of size.

size of the microplastics. When the size of the microplastics is reduced, the reduction in the volume of the microplastics leads to weaker Raman signal intensity, but it is more conducive for the microplastics to penetrate into the nanopores. In our previous studies, the V-shaped nanostructure has a significant enhancement effect in the nanopores. Therefore, when the Raman intensity decrease caused by the volume change is less than the Raman intensity increase caused by the position change, it will cause the result that the EFs increase with the decrease of the particle size.

Comparing Fig. 4(g) with Fig. 5(g), the EFs of each size of PS microspheres are all prior than that of PMMA. It can be interpreted as weaker normal Raman cross section and lower sensitivity to the AuNPs@V-shaped AAO SERS substrate of PMMA (Heller et al., 2016). Furthermore, the two sputtering methods produced different values of EF. In this work, the substrate formed by magnetron sputtering always achieved a higher EF than the substrate prepared by ion sputtering. This rule is consistent in the PS and PMMA detection. We can relate this conclusion to the morphological distribution of

AuNPs formed by the two sputtering methods. According to Fig. 2, the AuNPs formed by ion sputtering were larger in size and seem to form agglomerates. On the contrary, the AuNPs formed by magnetron sputtering were finer and smoother, which may provide a more uniform "hot spot" array.

3.6 SERS detection and identification of microplastics in rainwater

In addition to testing lab samples, we also collected real atmospheric aerosol samples to investigate the practical application capabilities of AuNPs@V-shaped AAO SERS substrate as well as detection and identification of microplastic particles in real environment. In this work, rainwater was collected at Fudan University (China) and treated as described in Materials and methods. Figure 6(a) shows the optical microscopy image of the selected particle, and Fig. 6(b) provides the corresponding Raman spectra. According to the scale bar in Fig. 6(a), the size of the selected particle was about 2 μm × 2 μm. Despite the interference from some impurity, the peaks marked in Fig. 6(b) were coincide with the characteristic peaks of PS, especially at 1003 cm^{-1} and 1033 cm^{-1}. Therefore, we can identify the selected particles as PS particles. It proved that AuNPs@V-shaped AAO SERS substrate was feasible and promising for ambient microplastics identification. It is noteworthy that there remains challenges in small-size microplastics researches in spite of recent many studies on identification of microplastics. Therefore, the proposal of AuNPs@V-shaped AAO SERS substrate provides a new idea for the subsequent development of small-size microplastics researches.

3.7 Discussion on AuNPs@V-shaped AAO SERS substrate

In our previous work, we have proved that SERS substrate with specialized inverted-pyramid structure has strong SERS performance due to a combined surface and volume electric filed enhancement. According to the results of electric field distribution simulations based on the finite-difference time-domain (FDTD) method, we found that E-field hotspots were strongly localized toward the bottom of the nanopores and close to the edges (Fu et al., 2017). Besides, nanostructure of V-shaped AAO template itself can introduce a little additional Raman scattering enhancement (He et al., 2019).

Comparing AuNPs@V-shaped AAO SERS substrate with Klarite, although they have similar inverted-cone nanostructure and the same metal NPs, their SERS performance in microplastics detection are significantly different. Klarite is prior in SERS performance and detection limits of microplastics. In this work, it is difficult to detect small nanoplastic with size of hundred nanometers. However, Klarite can realize detection of nanoplastics as small as 360 nm with much higher EF factors (Xu et al., 2020). The reasons for the above can be demonstrated as follows. First, the average top diameter of V-shaped AAO nanopores is about 400 nm, while that of Klarite is about 1.5 μm. The larger nanopore size of Klarite enables the microplastic particles to get inside, where the E-field hotspots are strongest. However, AuNPs@V-shaped AAO SERS substrate only allows part of Raman scattering of the microplastics affected by enhanced E-field. Second, the deposition of metal NPs upon the nanostructure has an important influence on SERS performance. The deposition methods adopted in this work may lead to disordered metal NPs deposition on nanostructure and poor long-range periodicity. Randomly aggregated metal NPs or disordered structure could hinder the plasmonic coupling effects of the ordered structure (Zhao et al., 2015).

Considering the real application situation, the AuNPs@V-shaped AAO SERS substrate proposed in this work provides a much lower cost approach for the large-scale detection of microplastics. In that case, Klarite may not be necessarily the prior choice because it is expensive to manufacture and repeated use of Klarite will reduce its SERS performance. In the following work, the AuNPs@V-shaped AAO SERS substrate can be further improved.

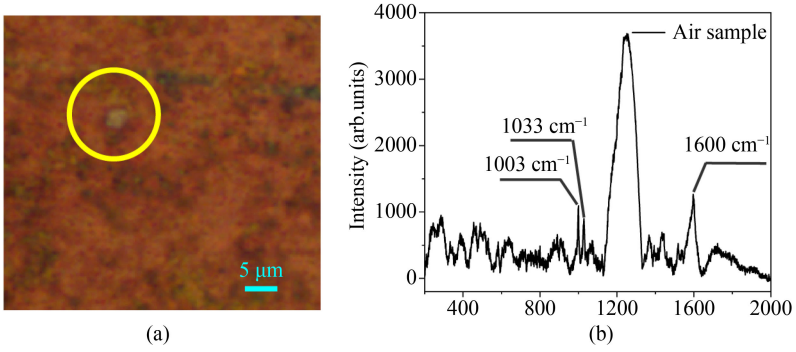

Fig. 6 (a) Optical, bright-field microscopy image of the particles identified as PS on AuNPs@V-shaped AAO SERS substrate (the size was about 2 μm × 2 μm); (b) Raman spectra of particles identified as PS from ambient atmospheric samples extracted in Shanghai (China) (5 spectral accumulations × 50 s acquisition time).

First, other metal deposition methods that can make the metal NPs form a more uniform distribution can be considerd. Second, incident laser wavelength is significantly related to the electric field distribution. Therefore, we can utilize different laser wavelength to transform the electric field distribution for better SERS performance. Third, changing noble metal NPs, such as silver, may obtain a higher Raman signal.

4 Conclusions

A new SERS substrate of low cost for small sized microplastic detection was developed by ion sputtering or magnetron sputtering AuNPs on the V-shaped AAO template. The results show AuNPs@V-shaped AAO SERS substrate has certain advantages in the detection of microplastics as small as 1 μm at the level of a single particle. The enhancement factor of AuNPs@V-shaped AAO SERS substrate for a single microplastic of different sizes and types can reach up to 20 (in detecting a single 2 μm PS sphere). In addition to the contribution of three-dimensional AuNPs structure to SERS enhancement, the inverted cone-shaped nanopore array could provide additional volume enhancement. According to SEM images and Raman spectra, AuNPs@V-shaped AAO SERS substrate formed by magnetron sputtering was compared with that formed by ion sputtering. Two sputtering methods formed completely different gold nanotopographies respectively and thus caused differences in the SERS analysis of microplastics. SERS substrate formed by magnetron sputtering obtained higher EF results in the detection of PS and PMMA, indicating that magnetron sputtering was more suitable. The substrate was also successfully applied to detect microplastics (about 2 μm × 2 μm in size) in rainwater.

Although this work demonstrates the potential of AuNPs@V-shaped AAO SERS substrate for small-size microplastics detection, further researches are still needed to achieve better goals. First of all, SERS analysis is suitable for the detection of nanoplastics according to some studies. In our previous work, the detectable size of one single nanoplastic particle by SERS analysis has reached 360 nm, which was based on a commercial SERS substrate named Klarite. Although the current stable detectable size of microplastic particles based on AuNPs@V-shaped AAO SERS substrate was 1 μm, the substrate has advantages in cost control and large scale production. In subsequent research, the substrate need to be further explored and optimized to achieve stable, efficient and sensitive detection of nanoplastics. Second, due to the complexity of the composition of the ambient samples, Raman signal from target substance is difficult to be distinguished from the fluorescence background signal produced by other impurities. Third, one of the significant challenges from SERS substrate is to produce and maintain consistent and uniform “hot spots” of electric field enhancement. Therefore, AuNPs@V-shaped AAO SERS substrate needs to be further developed to obtain a better SERS performance. Last but not least, quantitative analysis of small-size microplastics and even nanoplastics remains significant challenges, which call for more advanced technologies and thus provide methodological support for studying properties and impact of microplastics.

Acknowledgements The authors gratefully acknowledge financial support from the National Natural Science Foundation of China (Nos. 22176036, 21976030 and 22006020), the Natural Science Foundation of Shanghai (China) (No. 19ZR1471200).

References

Anema J R, Brolo A G, Felten A, Bittencourt C (2010). Surface-enhanced Raman scattering from polystyrene on gold clusters. Journal of Raman Spectroscopy, 41(7): 745–751

Araujo C F, Nolasco M M, Ribeiro A M P, Ribeiro-Claro P J A (2018). Identification of microplastics using Raman spectroscopy: Latest developments and future prospects. Water Research, 142: 426–440

Bergmann M, Wirzberger V, Krumpen T, Lorenz C, Primpke S, Tekman M B, Gerdts G (2017). High quantities of microplastic in arctic deep-sea sediments from the HAUSGARTEN observatory. Environmental Science & Technology, 51(19): 11000–11010

Catarino A I, Macchia V, Sanderson W G, Thompson R C, Henry T B (2018). Low levels of microplastics (MP) in wild mussels indicate that MP ingestion by humans is minimal compared to exposure via household fibres fallout during a meal. Environmental Pollution, 237: 675–684

Chen G, Feng Q, Wang J (2020). Mini-review of microplastics in the atmosphere and their risks to humans. Science of the Total Environment, 703: 135504

Foulon V, Le Roux F, Lambert C, Huvet A, Soudant P, Paul-Pont I (2016). Colonization of polystyrene microparticles by vibrio crassostreae: Light and electron microscopic investigation. Environmental Science & Technology, 50(20): 10988–10996

Fu Y, Kuppe C, Valev V K, Fu H, Zhang L, Chen J (2017). Surface-enhanced Raman spectroscopy: A facile and rapid method for the chemical component study of individual atmospheric aerosol. Environmental Science & Technology, 51(11): 6260–6267

He S, Xie W, Fang S, Huang X, Zhou D, Zhang Z, Du J, Du C, Wang D (2019). Silver films coated inverted cone-shaped nanopore array anodic aluminum oxide membranes for SERS analysis of trace molecular orientation. Applied Surface Science, 488: 707–713

Heller E J, Yang Y, Kocia L, Chen W, Fang S, Borunda M, Kaxiras E (2016). Theory of graphene raman scattering. ACS Nano, 10(2): 2803–2818

Hendrickson E, Minor E C, Schreiner K (2018). Microplastic abundance and composition in western lake superior as determined via microscopy, Pyr-GC/MS, and FTIR. Environmental Science & Technology, 52(4): 1787–1796

Huang D, Tao J, Cheng M, Deng R, Chen S, Yin L, Li R (2021).

Microplastics and nanoplastics in the environment: Macroscopic transport and effects on creatures. Journal of Hazardous Materials, 407: 124399

Koelmans A A, Bakir A, Burton G A, Janssen C R (2016). Microplastic as a vector for chemicals in the aquatic environment: Critical review and Model-Supported reinterpretation of empirical studies. Environmental Science & Technology, 50(7): 3315–3326

Koelmans A A, Mohamed Nor N H, Hermsen E, Kooi M, Mintenig S M, De France J (2019). Microplastics in freshwaters and drinking water: Critical review and assessment of data quality. Water Research, 155: 410–422

Langer J, Jimenez de Aberasturi D, Aizpurua J, Alvarez-Puebla R A, Auguié B, Baumberg J J, Bazan G C, Bell S E J, Boisen A, Brolo A G, et al. (2020). Present and future of surface-enhanced Raman scattering. ACS Nano, 14(1): 28–117

Law K L, Thompson R C (2014). Microplastics in the seas. Science, 345(6193): 144–145

Lê Q T, Ly N H, Kim M K, Lim S H, Son S J, Zoh K D, Joo S W (2021). Nanostructured Raman substrates for the sensitive detection of submicrometer-sized plastic pollutants in water. Journal of Hazardous Materials, 402: 123499

Liu K, Wu T, Wang X, Song Z, Zong C, Wei N, Li D (2019). Consistent transport of terrestrial microplastics to the ocean through atmosphere. Environmental Science & Technology, 53(18): 10612–10619

Lv L, He L, Jiang S, Chen J, Zhou C, Qu J, Lu Y, Hong P, Sun S, Li C (2020). In situ surface-enhanced Raman spectroscopy for detecting microplastics and nanoplastics in aquatic environments. Science of the Total Environment, 728: 138449

Mohamed Nor N H, Kooi M, Diepens N J, Koelmans A A (2021). Lifetime accumulation of microplastic in children and adults. Environmental Science & Technology, 55(8): 5084–5096

Nagaura T, Takeuchi F, Inoue S (2008). Fabrication and structural control of anodic alumina films with inverted cone porous structure using multi-step anodizing. Electrochimica Acta, 53(5): 2109–2114

Parker J, Feldman D, Ashkin M (1967). Raman scattering by silicon and germanium. Physical Review, 155(3): 712–714

Ragusa A, Svelato A, Santacroce C, Catalano P, Notarstefano V, Carnevali O, Papa F, Rongioletti M C A, Baiocco F, Draghi S, D' Amore E, Rinaldo D, Matta M, Giorgini E (2021). Plasticenta: First evidence of microplastics in human placenta. Environment International, 146: 106274

Rillig M C, Lehmann A (2020). Microplastic in terrestrial ecosystems. Science, 368(6498): 1430–1431

Schwabl P, Köppel S, Königshofer P, Bucsics T, Trauner M, Reiberger T, Liebmann B (2019). Detection of various microplastics in human stool: A prospective case series. Annals of Internal Medicine, 7(171): 453–457

Seeley M E, Song B, Passie R, Hale R C (2020). Microplastics affect sedimentary microbial communities and nitrogen cycling. Nature Communications, 11(1): 2372

Shi G, Wang M, Zhu Y, Yan X, Pan S, Zhang A (2019). Nanoflower-like Ag/AAO SERS platform with quasi-photonic crystal nanostructure for efficient detection of goat serum. Current Applied Physics, 19(11): 1276–1285

Tekman M B, Wekerle C, Lorenz C, Primpke S, Hasemann C, Gerdts G, Bergmann M (2020). Tying up loose ends of microplastic pollution in the arctic: Distribution from the sea surface through the water column to deep-sea sediments at the HAUSGARTEN observatory. Environmental Science & Technology, 54(7): 4079–4090

Thompson R C, Olsen Y, Mitchell R P, Davis A, Rowland S J, John A W, McGonigle D, Russell A E (2004). Lost at sea: where is all the plastic? Science, 304(5672): 838

Wang C, Zhao J, Xing B (2021). Environmental source, fate, and toxicity of microplastics. Journal of Hazardous Materials, 407: 124357

Wang L, Zhang J, Hou S, Sun H (2017). A simple method for quantifying polycarbonate and polyethylene terephthalate microplastics in environmental samples by liquid chromatography–tandem mass spectrometry. Environmental Science & Technology Letters, 4(12): 530–534

Wang X, Huang S, Hu S, Yan S, Ren B (2020). Fundamental understanding and applications of plasmon-enhanced Raman spectroscopy. Nature Reviews Physics, 2(5): 253–271

Xu G, Cheng H, Jones R, Feng Y, Gong K, Li K, Fang X, Tahir M A, Valev V K, Zhang L (2020). Surface-enhanced Raman spectroscopy facilitates the detection of microplastics < 1 μm in the environment. Environmental Science & Technology, 54(24): 15594–15603

Zhang Q, Xu E G, Li J, Chen Q, Ma L, Zeng E Y, Shi H (2020a). A review of microplastics in table salt, drinking water, and air: Direct human exposure. Environmental Science & Technology, 54(7): 3740–3751

Zhang Y, Pu S, Lv X, Gao Y, Ge L (2020b). Global trends and prospects in microplastics research: A bibliometric analysis. Journal of Hazardous Materials, 400: 123110

Zhao J, Lin J, Li X, Zhao G, Zhang W (2015). Silver nanoparticles deposited inverse opal film as a highly active and uniform SERS substrate. Applied Surface Science, 347: 514–519

Zhu X, Huang W, Fang M, Liao Z, Wang Y, Xu L, Mu Q, Shi C, Lu C, Deng H, Dahlgren R, Shang X (2021). Airborne microplastic concentrations in five megacities of northern and southeast China. Environmental Science & Technology, 55(19): 12871–12881